Activity-dependent and -independent nuclear fluxes of HDAC4 mediated by different kinases in adult skeletal muscle

Yewei Liu,[1] William R. Randall,[2] and Martin F. Schneider[1]

[1]Department of Biochemistry and Molecular Biology and [2]Department of Pharmacology and Experimental Therapeutics, University of Maryland School of Medicine, Baltimore, MD 21201

Class II histone deacetylases (HDACs) may decrease slow muscle fiber gene expression by repressing myogenic transcription factor myocyte enhancer factor 2 (MEF2). Here, we show that repetitive slow fiber type electrical stimulation, but not fast fiber type stimulation, caused HDAC4-GFP, but not HDAC5-GFP, to translocate from the nucleus to the cytoplasm in cultured adult skeletal muscle fibers. HDAC4-GFP translocation was blocked by calmodulin-dependent protein kinase (CaMK) inhibitor KN-62. Slow fiber type stimulation increased MEF2 transcriptional activity, nuclear Ca^{2+} concentration, and nuclear levels of activated CaMKII, but not total nuclear CaMKII or CaM-YFP. Thus, calcium transients for slow, but not fast, fiber stimulation patterns appear to provide sufficient Ca^{2+}-dependent activation of nuclear CaMKII to result in net nuclear efflux of HDAC4. Nucleocytoplasmic shuttling of HDAC4-GFP in unstimulated resting fibers was not altered by KN-62, but was blocked by staurosporine, indicating that different kinases underlie nuclear efflux of HDAC4 in resting and stimulated muscle fibers.

Introduction

In skeletal muscle, activity-dependent expression of slow or oxidative fiber type–specific genes may be mediated by the transcription factors myocyte enhancer factor 2 (MEF2; Black and Olson, 1998; Wu et al., 2000) and nuclear factor of activated T cells (NFAT; Chin et al., 1998). According to several recent papers, MEF-2 forms a complex with members of the class II histone deacetylase (HDAC; HDACs 4, 5, 7, and 9) family of proteins within the nucleus in a variety of cell types, including skeletal muscle, which represses transcriptional activation by MEF-2 (Miska et al., 1999).

The repression of MEF2 transcriptional activation by class II HDACs is regulated by the phosphorylation status of HDAC in a variety of cell types. Dephosphorylated HDAC remains within the nucleus and represses MEF2 activity. In response to activation of calmodulin-dependent protein kinase (CaMK), HDAC becomes phosphorylated (Kao et al., 2001). Phosphorylated HDAC binds to the chaperone protein 14-3-3 (Van Hemert et al., 2001) within the nucleus and moves out of the nucleus via the nuclear export protein CRM1 in complex with 14-3-3 (Grozinger and Schreiber, 2000; McKinsey et al., 2001). HDAC removal from the nucleus would eliminate HDAC inhibition of MEF2 activation of gene expression. Class II HDACs distribute between the nucleus and the cytoplasm depending on the activity of CaMK (McKinsey et al., 2000a). The intra-nuclear phosphorylation of HDAC by CaMK and resulting nuclear efflux of HDAC thus provides a possible Ca^{2+} pattern–dependent, phosphorylation-mediated signaling pathway for regulation of slow fiber type gene expression in muscle.

We now use cultured adult skeletal muscle fibers to investigate the activity-dependent nucleocytoplasmic translocation of HDAC4-GFP in response to different stimulation frequencies, as well as the activity-dependent and the resting translocation of HDAC4-GFP in the presence of different kinase, phosphatase, or transport inhibitors. We find that 10-Hz train stimulation to mimic slow-twitch fiber activity (Hennig and Lomo, 1985) caused net nuclear to cytoplasmic translocation of HDAC4-GFP, but not of HDAC5-GFP. Translocation of HDAC4-GFP resulting from electrical stimulation was completely blocked by the CaMK inhibitor KN-62. This stimulation pattern also increased nuclear levels of activated CaMKII and increased MEF2 transcription activity. Blocking of the nuclear export system in unstimulated fibers resulted in net nuclear HDAC4-GFP accumulation, indicative of active nucleocytoplasmic shutting of HDAC4 in resting fibers. However, the subcellular distribution of HDAC4-GFP was not affected

Correspondence to M.F. Schneider: mschneid@umaryland.edu

Abbreviations used in this paper: AOI, areas of interest; CaMK, calmodulin-dependent protein kinase; CsA, cyclosporin A; FDB, flexor digitorum brevis; HDAC, histone deacetylase; MEF2, myocyte enhancer factor 2; NFAT, nuclear factor of activated T cells.

The Journal of Cell Biology, Vol. 168, No. 6, March 14, 2005 887–897
http://www.jcb.org/cgi/doi/10.1083/jcb.200408128

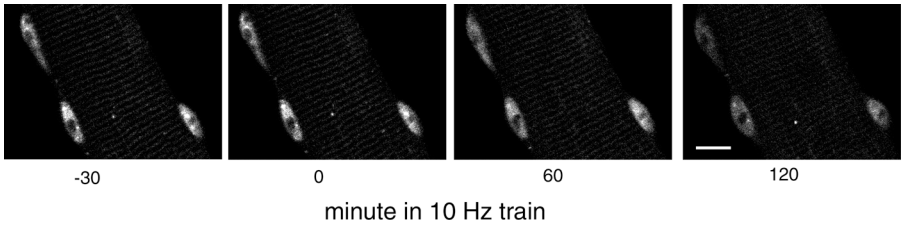

Figure 1. **Images of a fiber expressing HDAC4-GFP before and during stimulation with 10-Hz trains.** A fiber expressing HDAC4-GFP is shown in Ringer's solution at RT 30 min before stimulation (−30), at the start of stimulation (0), and after stimulation for 60 or 120 minutes with 5-s duration trains of 10-Hz pulses applied every 50 s. After 2-h stimulation there is a significant decline of fluorescence in all the nuclei. Bar, 10 μm.

by KN-62 in resting fibers. Thus, different phosphorylation/dephosphorylation mechanisms underlie the resting shuttling and the activity-dependent nuclear efflux of HDAC4 in skeletal muscle.

Results

Intracellular distribution of HDAC4-GFP

HDAC4-GFP fusion protein was present in both the cytoplasm in a sarcomeric pattern and nucleus of fully differentiated adult flexor digitorum brevis (FDB) skeletal muscle fibers in culture after transduction with adenovirus and expression for ∼3 d (Fig. 1). The mean value of the ratio of nuclear to cytoplasmic mean pixel fluorescence was 2.4 ± 0.2 (28 nuclei from 16 HDAC4-GFP–infected fibers). Hemagglutinin-tagged HDAC4 (HDAC4-HA) showed a similar pattern of distribution as HDAC4-GFP–infected and immunostained FDB fibers (unpublished data). HDAC4-GFP–infected FDB fibers exhibited variable numbers of 1–2-μm-long elongated inclusion bodies in the cytoplasm (Kirsh et al., 2002), generally oriented parallel to the fiber axis, as did HDAC4-HA–infected fibers stained with anti-HA antibody (unpublished data). Thus, these inclusion bodies result from HDAC4 and not the GFP moiety. Inclusion bodies were not included in analyzing the fluorescence of cytoplasmic HDAC4-GFP. Self-aggregation of HDAC4 both in the cytoplasm and nucleus of other cell types has been reported previously, possibly due to an NH_2-terminal HDAC4 dimerization domain and sumolyation of HDAC4 (Kirsh et al., 2002).

Activity-dependent translocation of HDAC4-GFP

Next, we investigated translocation of HDAC4-GFP from the nucleus to the cytoplasm in response to electrical stimulation patterns mimicking the physiological activity patterns of skeletal muscle. After 30 min without stimulation, during which the fluorescence in both the nucleus and the cytoplasm was stable (Fig. 1, −30 and 0 min), fibers were repeatedly stimulated with a 10-Hz train for 5 s every 50 s. Field stimulation resulted in visible twitches throughout the period of stimulation in all fibers used for analysis. This electrical stimulation caused a noticeable translocation of HDAC4-GFP from the nucleus to the cytoplasm (Fig. 1, 60 and 120 min). Over a 2-h period of repetitive stimulation (5-s duration 10-Hz trains every 50 s) nuclear fluorescence continuously decreased, indicating continued net translocation of HDAC4-GFP out of the nucleus. This net efflux of HDAC4-GFP from the nucleus occurred without any significant change in cytoplasmic fluorescence (Fig. 2 A), indicating that the total cytoplasmic pool of HDAC4-GFP was much larger than the size of the total nuclear pool.

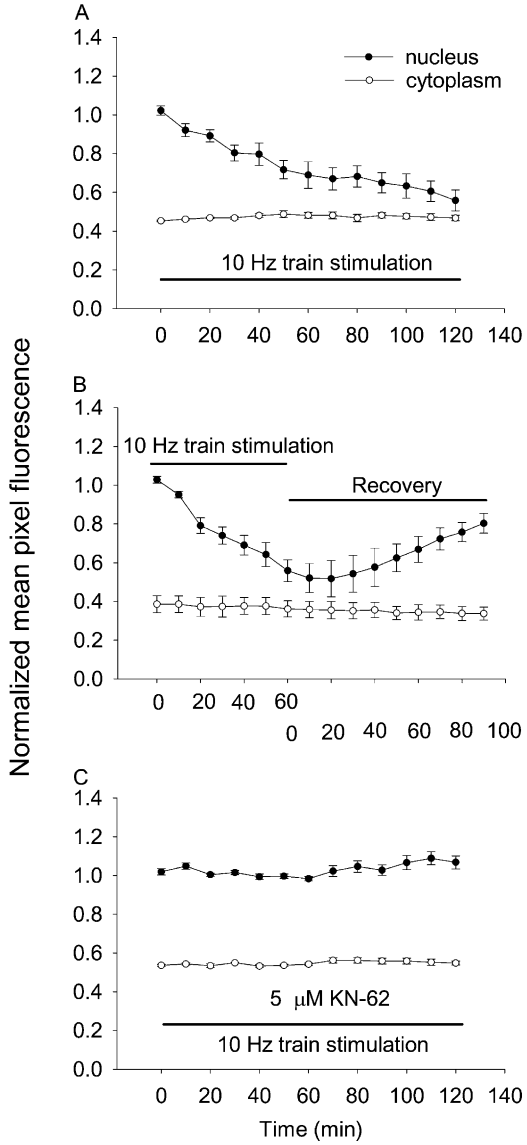

Figure 2. **Time course of nuclear to cytoplasmic translocation of HDAC4 during 10-Hz train stimulation.** (A) The average fluorescence intensity per pixel over whole nuclei (closed circles) or over the cytoplasm (open circles) was quantitated and normalized as described in Materials and methods. 5-s trains of 10-Hz stimuli every 50 s resulted in net nuclear to cytoplasmic translocation of HDAC4-GFP. Nuclear fluorescence declined continuously during the 120-min stimulation period. The cytoplasmic fluorescence remained constant during the same period of time. (B) The reversibility of HDAC4-GFP efflux due to electrical stimulation. (C) CaMK inhibitor KN-62 blocked the nuclear to cytoplasmic translocation of HDAC4-GFP in stimulated fibers.

The efflux of HDAC4-GFP in response to electrical stimulation was reversible. Fibers infected with HDAC4-GFP were stimulated with 10-Hz trains for 1 h during which HDAC4-GFP translocated from the nucleus to the cytoplasm (Fig. 2 B). The stimulation was then stopped. Nuclear HDAC4-GFP fluorescence continued to drop for ~10–20 min after the end of stimulation, possibly indicating delayed reversal of CaMKII activation. Subsequently, the nuclear fluorescence began to increase. By 90 min after the electrical stimulation was terminated, the nuclear HDAC4-GFP had recovered to 75% of the value before electrical stimulation, with a steady trend of continuing influx of HDAC4-GFP at the end of the monitoring interval (eight nuclei from four fibers).

It is known that CaMK can phosphorylate class II HDACs (Grozinger and Schreiber, 2000; Wang et al., 2000). Phosphorylated intranuclear HDACs bind to 14-3-3 proteins (McKinsey et al., 2001), exposing a nuclear export signal at the HDAC COOH terminus and thus allowing HDAC translocation to the cytoplasm. Therefore, we equilibrated fibers with the CaMK inhibitor KN-62 (5 μM, a concentration selective for CaM kinase inhibition; Tokumitsu et al., 1990; Deisseroth et al., 1996) for 30 min without stimulation, and then stimulated with 10-Hz trains for 5 s every 50 s. In the presence of 5 μM KN-62, there was no change in either nuclear or cytoplasmic fluorescence either at rest or in response to 10-Hz train stimulation (Fig. 2 C; nine nuclei from four fibers). The results in Fig. 2 (A and C) strongly suggest that electrical stimulation resulted in HDAC4-GFP phosphorylation by CaMK before translocation.

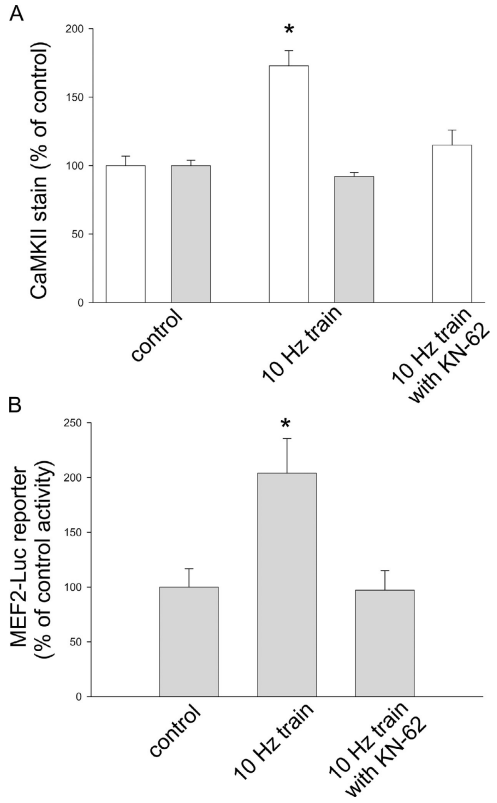

Figure 3. **Effect of stimulation on CaMKII phosphorylation and MEF2 reporter activity.** (A) Mean nuclear pixel fluorescence (normalized to control) in resting fibers and fibers repeatedly stimulated for 1 h using 10-Hz trains in the presence or absence of KN-62 and labeled with antibody for either autophosphorylated (open bars) or total (closed bars) CaMKII. Only nuclei stimulated in the absence of KN-62 and stained for autophosphorylated CaMKII exhibited a significant increase in nuclear staining after stimulation. From left to right, the data were averages of mean nuclear fluorescence from 26, 17, 23, 21, or 13 nuclei from 22, 12, 18, 12, or 10 fibers, respectively. (B) Luciferase activity was increased in fibers infected with adenovirus-encoding MEF2-luciferase reporter and stimulated with 10-Hz trains for 5 h. 5 μM KN-62 blocked the increase in luciferase activity stimulated with 10-Hz trains. Results represent triplicate measurements from each of three independent experiments. Error bars represent ± 1 SEM. *, $P < 0.05$ versus control without stimulation.

Activation of nuclear CaMKII and MEF2

To test for changes in CaMKII phosphorylation, fibers were stimulated with a 5-s duration 10-Hz train every 50 s for 1 h with or without 5 μM KN-62 in the Ringer's solution and fixed and stained with primary antibody to activated (autophosphorylated; Fig. 3 A, open bars) or total (Fig. 3 A, filled bars) CaMKII. 1 h of 10-Hz train stimulation significantly increased ($P < 0.01$) the mean nuclear stain of activated CaMKII compared with unstimulated fibers, and KN-62 (5 μM) blocked the increase in activated CaMKII staining after stimulation (Fig. 3 A). In parallel experiments, in which the fibers were stained with antibody directed against total CaMKII, there was no difference in mean nuclear antibody stain between stimulated and unstimulated fibers ($P > 0.05$; Fig. 3 A). These results are consistent with activation of nuclear CaMKII by fiber electrical stimulation without any appreciable translocation of CaMKII from the cytoplasm to the nucleus.

10-Hz train stimulation also caused changes in expression of a MEF2-driven luciferase reporter introduced into the fibers via an adenoviral construct (Wilkins et al., 2004). 5 h of repetitive stimulation (5-s duration 10-Hz trains every 50 s) followed by 19 h without stimulation caused luciferase activity in fiber culture extracts to approximately double compared with extracts from parallel unstimulated fiber cultures (Fig. 3 B). The same stimulation (5 h, followed by 19 h without stimulation) in the presence of the CaMK inhibitor KN-62 gave the same luciferase activity as control. Thus, KN-62 completely blocked the stimulation-dependent increase in MEF2 reporter activity, just as KN-62 completely blocked the stimulation-dependent efflux of HDAC4 from the nucleus (Fig. 2).

Effects of stimulation patterns on nuclear efflux of HDAC4

1-Hz continuous stimulation also caused the exit of HDAC4-GFP from the nucleus (Fig. 4 A), but the efflux was somewhat lower than with the 10-Hz trains. Using linear fits to the data from each fiber, the mean initial net export rate during the first 30 min of 1-Hz continuous stimulation was −0.45 ± 0.10%/min over (10 nuclei from 5 fibers), which is slower than the corresponding value of −0.62 ± 0.12%/min obtained from the fibers stimulated with 5-s 10-Hz trains every 50 s (Fig. 2 A; 10 nuclei from 6 fibers). In contrast to the 10-Hz train stimulation (Fig. 2 A), which is typical for slow type fibers, using 100-ms trains at 100 Hz every 50 s, which is a typical pattern of fast fiber type activity (Hennig and Lomo, 1985), did not cause any detectable change in nuclear fluorescence, indicating negligible net nucleus to cytoplasm translocation of HDAC4-GFP with the fast fiber type stimulation pattern

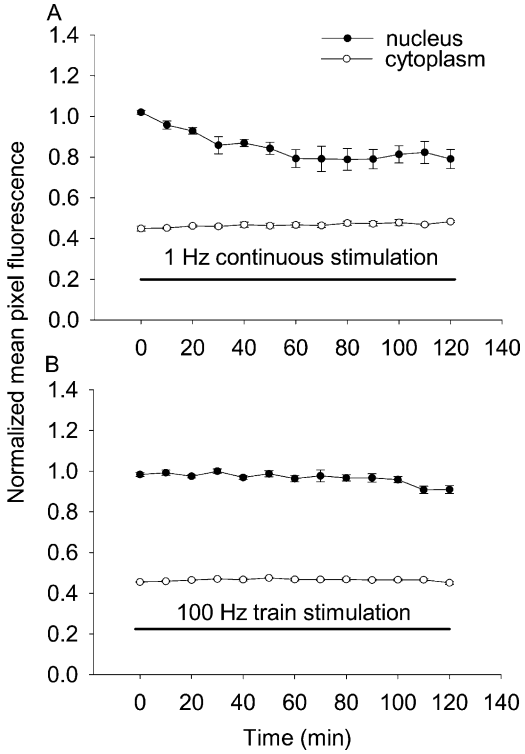

Figure 4. **Time course of nuclear to cytoplasmic translocation of HDAC4 with 1- or 100-Hz stimulation.** (A) 1-Hz continuous stimulation resulted in nuclear to cytoplasmic translocation of HDAC4-GFP, but with a lower mean initial net export rates compared with 10-Hz trains. The 10-Hz trains were more effective than 1 Hz in causing HDAC4-GFP nuclear export. Nuclear fluorescence declined continuously during the 120-min stimulation period. The cytoplasmic fluorescence remained constant during the same period of time. (B) 100-ms train at 100 Hz every 50 s did not have effects on the subcellular distribution of HDAC4-GFP.

(Fig. 4 B, eight nuclei from six fibers). Thus, we conclude that the rate and extent of loss of nuclear HDAC4 is determined by the pattern of activity experienced by the muscle fibers, and that the typical slow pattern of stimulation, but not the fast pattern, induces nuclear to cytoplasmic translocation of HDAC4.

Subcellular distribution of HDAC5-GFP was not altered by electrical stimulation

Both HDAC4 and HDAC5 are class II histone deacetylases, exhibiting high levels of expression in skeletal muscle and involvement in muscle differentiation (Lu et al., 2000; McKinsey et al., 2000a). Fibers expressing HDAC5-GFP were repetitively stimulated with 10-Hz trains for 5 s every 50 s, as in fibers expressing HDAC4-GFP. Surprisingly, 2 h of 10-Hz train stimulation, which resulted in ~49% drop of nuclear HDAC4-GFP, decreased the nuclear HDAC5-GFP by only 11% (Fig. 5, A and B, 10 nuclei from 5 fibers), suggesting a significant difference between HDAC4 and HDAC5 in the sensitivity to the electrical stimulation. Another difference between HDAC4 and 5-GFP was that under resting conditions without electrical stimulation, the mean value of the ratio of cytoplasmic to nuclear mean pixel fluorescence was 51 ± 4% for HDAC4-GFP (28 nuclei from 16 fibers) but only 13 ± 2% for HDAC5-GFP (31 nuclei from 17 fibers), indicating more effective nuclear retention of HDAC5.

Calmodulin-YFP distribution is not altered by electrical stimulation

Because CaMK appears to mediate the stimulation-dependent translocation of HDAC4 from the nucleus to the cytoplasm (Fig. 2), we next examined the intracellular distribution of CaM-YFP, expressed by adenoviral infection, to see if stimulation recruited CaM to the nucleus. In resting fibers, CaM-YFP exhibited a sarcomeric pattern in the cytoplasm, with the bright lines in the pattern corresponding to α-actinin localization at the Z line (not depicted), and a diffuse pattern in the nucleus except the nucleolus (Fig. 6 A). There was significant CaM-YFP in the A-band region between Z-lines, giving a pixel fluorescence about half that at the Z-line and indicating presence of CaM within the sarcomere away from the Z-line. The mean value of the ratio of nuclear to cytoplasmic mean pixel fluorescence was 0.79 ± 0.05 (11 nuclei from 7 fibers). This ratio was stable in resting fibers and did not change during a 2-h period of repetitive stimulation with 5-s trains of 10-Hz stimuli applied every

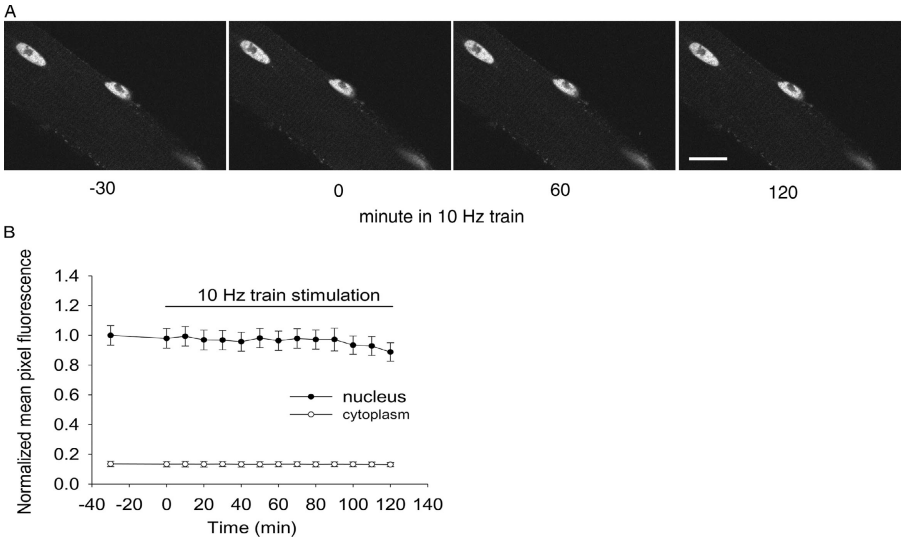

Figure 5. **There was no significant change in subcellular distribution of HDAC5-GFP in fibers stimulated with 10-Hz trains.** (A) A fiber expressing HDAC5-GFP is shown 30 min before (−30), at the start of (0), and after stimulation for 60 or 120 min. Because of the relatively low cytoplasmic HDAC5, only the nuclei are apparent. (B) The average fluorescent intensity per pixel over whole nuclei (closed circles) or over the cytoplasm (open circles) was quantitated and normalized. After 2 h of 10-Hz train stimulation, there was no significant decline of nuclear fluorescence. Bar, 10 μM.

50 s (Fig. 6 B, left), a stimulus pattern that produced clear KN-62-sensitive, stimulation-dependent translocation of HDAC4 from the nucleus to the cytoplasm (Fig. 2). CaM-YFP also did not exhibit any change in nuclear-cytoplasmic distribution during 2 h of continuous 1-Hz stimulation (Fig. 6 B, right).

We also performed CaM-YFP FRAP measurements to determine the rate of CaM-YFP nuclear movement. Fluorescence over the entire nucleus was significantly suppressed by photobleaching (Fig. 6 C), and the time course of subsequent fluorescence recovery in the nucleus was imaged in resting fibers (Fig. 6 C). Exponential fits to FRAP time courses gave a mean rate constant of 3.48 ± 0.26%/min (seven nuclei from seven fibers). Thus, less than ~3.5% redistribution of CaM should have occurred in the <1-min interval from preceding stimulation to imaging in Fig. 6 (A or B) if the FRAP rate in resting fibers was the same as after fiber stimulation.

To confirm that CaM-YFP did not enter nuclei during stimulation and then leave within the few seconds before image acquisition, we imaged fiber nuclei within 1 s after termination of a 5-s train of 10-Hz stimuli. There was no indication of increased nuclear CaM-YFP immediately (i.e., <1 s) after stimulation (unpublished data). Thus, the physiological CaM kinase activation that underlies the nuclear to cytoplasmic translocation of HDAC4 during electrical stimulation (Fig. 2) does not appear to involve translocation of CaM from the cytoplasm to the nucleus, but must involve Ca^{2+} activation of CaM already resident in the nucleus, presumably due to an elevated nuclear Ca^{2+} during fiber stimulation.

In contrast to the lack of effect of electrical stimulation on the distribution of CaM, prolonged continuous elevation of Ca^{2+} concentration by addition of ionomycin (2 μM) to the bathing solution (presumably elevating both cytosolic and nuclear Ca^{2+} concentration) did give rise to a delayed redistribution of CaM from the cytoplasm to the nucleus, resulting in an increase in the ratio of nuclear-cytoplasmic CaM-YFP mean pixel fluorescence from 0.67 ± 0.08 before ionomycin to 1.88 ± 0.18 after 10-min exposure to ionomycin.

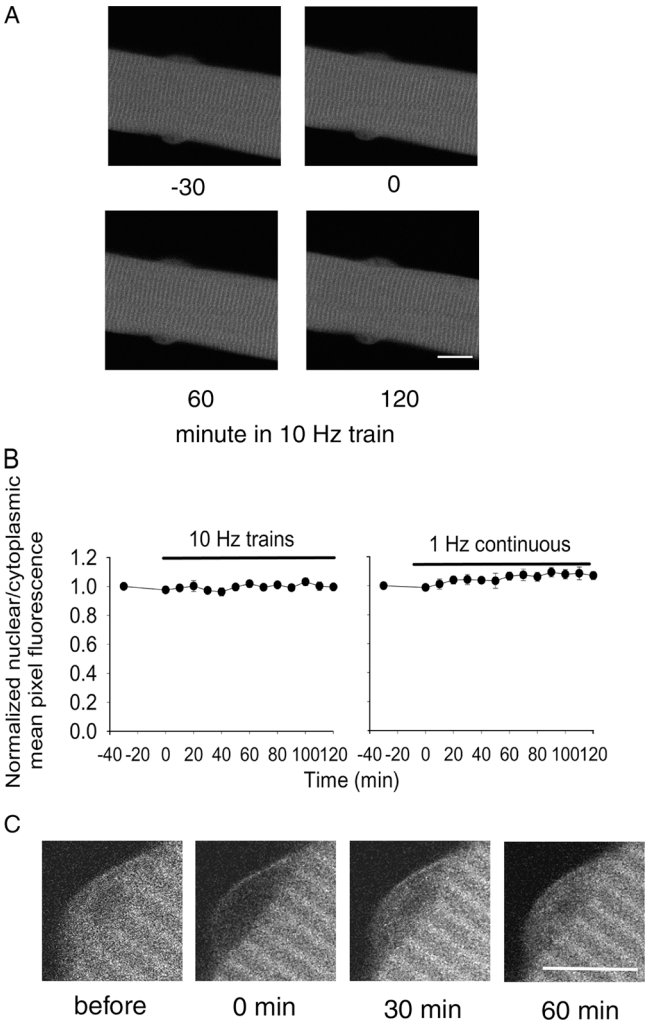

Figure 6. **The subcellular distribution of CaM-YFP was not changed by 10- or 1-Hz electrical stimulation.** (A) A typical living fiber expressing CaM-YFP is shown for 30 min (−30 and 0) before stimulation and 60 and 120 min after repetitive stimulation with 10-Hz trains. In resting fibers, CaM-YFP was present in the cytoplasm as well as the nucleus. (B) The fluorescence signals from both the nucleus and the cytoplasm were quantitated. Data are presented as the ratio of the average fluorescence intensity per pixel from the nucleus relative to the cytoplasm. Neither 10-Hz train stimulation (left) for 2 h nor 1-Hz continuous stimulation (right) resulted in any subcellular redistribution of CaM-YFP. (C) FRAP of CaM-YFP was performed in the nuclear area of a muscle fiber. Shown is a nucleus before photobleaching, immediately after photobleaching, and after 30 and 60 min of recovery. The entire nuclear region was selectively bleached. Bars, 10 μm.

Nuclear and cytoplasmic calcium is elevated during electrical stimulation

Muscle fibers loaded with the calcium indicator fluo-4 were imaged before, during, and after repetitive stimulation with 5-s duration 10-Hz trains applied every 50 s (Fig. 7 A). Note that full acquisition of each image in Fig. 7 A required 600 ms (top line first, bottom line last). Thus, when an image was acquired during the train (Fig. 7 A, b and f), the abrupt rise in fluorescence of the Ca^{2+} concentration indicator (sharp bright horizontal stripes across the fiber) in response to application of a given stimulus (Fig. 7 A, arrowheads) corresponds to a particular line that was imaged at a time when a stimulus was applied. The subsequent stimulus, applied 100 ms later in time, appears at a spatial location 5 μm further down the image because the images were acquired at 0.05 μm/ms. With the time resolution used here, each stimulus activates the entire fiber cross section essentially uniformly (Fig. 7 A, b and f). The decay of the cytosolic Ca^{2+} concentration signal occurs rapidly after the train of stimuli (Fig. 7 A, c; and Fig. 7 B), whereas nuclear Ca^{2+} concentration decays more slowly than cytosolic Ca^{2+} concentration (Fig. 7 B). The lower fluorescence of the nonratiometric Ca^{2+} indicator fluo-4 in the nucleus than in the cytoplasm in resting fibers (Fig. 7 B) probably does not indicate a difference in resting Ca^{2+} concentration, but more likely arises from preferential exclusion of dye from the nucleus, preferential binding of dye in the cytoplasm, lower affinity of the dye for Ca^{2+} in the nucleus than the cytoplasm, or a combination of these effects. Within the train of stimuli (Fig. 7 C), cytosolic Ca^{2+} concentration rises after each stimulus and then falls between pulses. In contrast, nuclear Ca^{2+} concentration seems to rise more slowly and continuously during the train (Fig. 7 B), as anticipated for diffusion of elevated Ca^{2+} concentration from the cytoplasm into the nucleus. Compared with the resting fiber (Fig. 7 A, a), nuclear

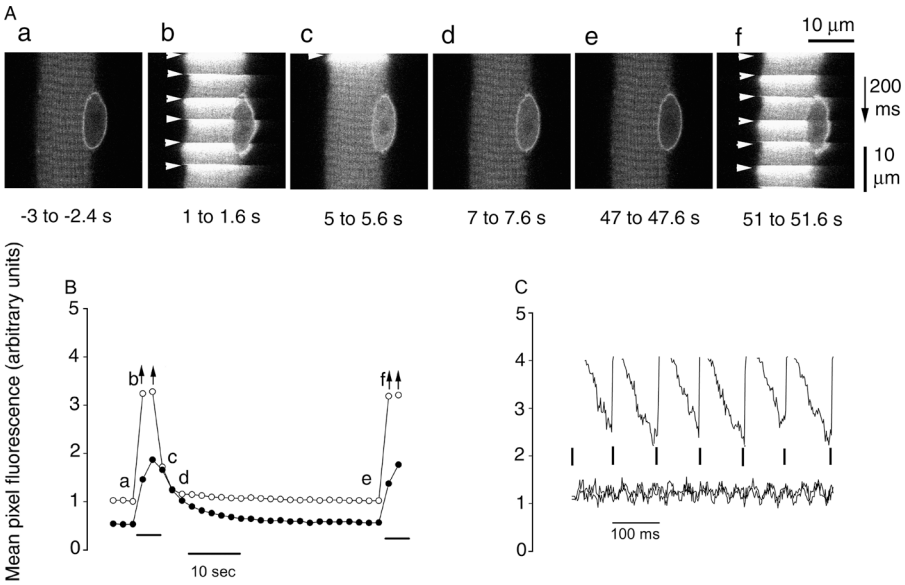

Figure 7. **Calcium concentration is elevated in both the nucleus and cytoplasm during repetitive electrical stimulation.** (A) A fiber was repetitively stimulated every 50 s with a 5-s duration train of pulses at 10 Hz. Calcium-dependent fluo-4 fluorescence images taken in x-y scan mode in the resting "control" condition before the start of repetitive stimulation (a), 1–1.6 s after the start of the first train (b), 0–0.6, 2–2.6, and 42–42.6 s after the first train (c–e), and 1–1.6 s after the start of the second train (f). The notched appearance at the edge of the fiber in panels b and f is due to individual nonfused fiber contraction at each stimulus. The nuclear Ca^{2+} concentration was still elevated compared with the rest a few hundred milliseconds after the end of the 5-s train (c). Arrowheads indicate the application of each stimulus within an image. Note that each image was scanned from top to bottom at 0.05 μm/ms. (B) Time course of nuclear (closed circles) or cytosolic (open circles) mean pixel fluorescence in the central 100 μm (recorded during 200 ms) of images in A and others not depicted. Arrows indicate underestimation of mean pixel fluorescence due to the inclusion of pixels maxed out due to detector saturation. Horizontal bars below records mark duration of the 5-s 10-Hz trains of stimuli. (C) Time course of cytoplasmic fluorescence from individual images (i.e., from top to bottom) during stimulation (top; from A, b) and before and after stimulation (bottom; from A, a and e). Vertical lines mark times of individual stimuli.

Ca^{2+} concentration remains elevated a few hundred ms after the end of the 5-s 10-Hz trains of pulses (Fig. 7 A, c; and Fig. 7 B). This elevated nuclear Ca^{2+} concentration then declines during the 45-s interval between successive trains (Fig. 7 B). Thus, activation of nuclear CaMK due to elevated nuclear Ca^{2+} concentration appears to be a likely mechanism underlying the CaMK-dependent HDAC4 efflux during fiber electrical stimulation.

Leptomycin B reveals shuttling of HDAC4 under resting conditions

Leptomycin B binds to the nuclear export mediator protein CRM1, thereby blocking the binding of CRM1 to proteins containing the nuclear export signal (Fukuda et al., 1997) and preventing their nuclear export. During exposure to leptomycin B (40 nM), nuclear HDAC4-GFP continuously increased over a 60-min experimental period, whereas the cytoplasmic fluorescence signal was stable (Fig. 8 A). Upon treatment with leptomycin B, HDAC4-GFP translocated into the nucleus at a constant rate (Fig. 8 B) of 0.88 ± 0.09%/min. Assuming that leptomycin B completely inhibited HDAC4 efflux from fiber nuclei, these results reveal a unidirectional influx of HDAC4 into nuclei at a rate of 0.88%/min. If influx was not altered by leptomycin B, then under resting conditions, before addition of leptomycin B and in the absence of

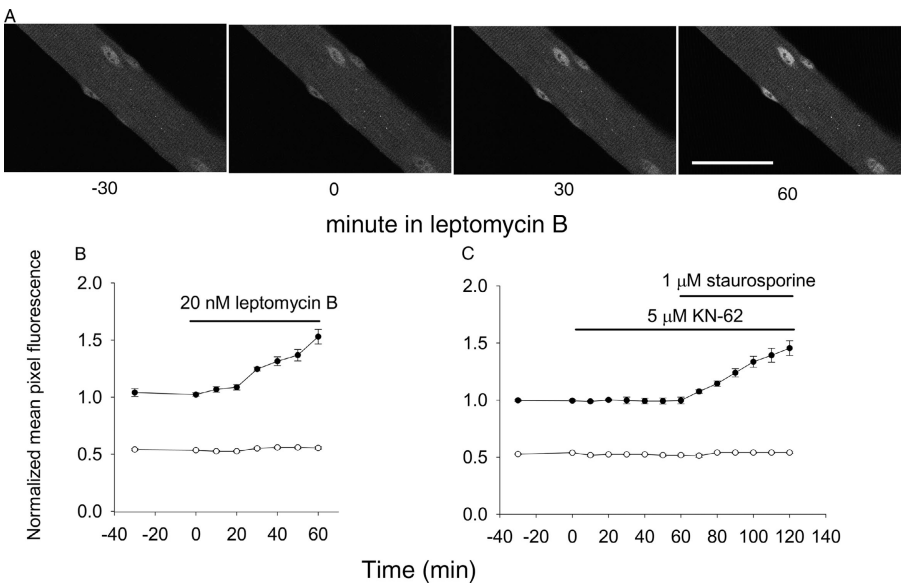

Figure 8. **Movements of HDAC4-GFP in unstimulated fibers in the presence of leptomycin B, KN-62, and staurosporine.** (A) A typical living fiber expressing HDAC4-GFP is shown in Ringer's solution without any treatment for 30 min (−30 and 0) and after 30 and 60 min in the presence of 40 nM leptomycin B, a specific inhibitor of the nuclear export receptor CRM1. In the presence of leptomycin B, nuclear HDAC4-GFP fluorescence was significantly increased. No changes in cytoplasmic fluorescence were detected. Bar, 50 μm. (B) Time course of nuclear and cytoplasmic HDAC4-GFP fluorescence before and during exposure to 20 nM leptomycin B. Leptomycin B block of nuclear export of HDAC4-GFP caused an increase of HDAC4-GFP in the nucleus. (C) KN-62 was first added to culture dishes with fibers expressing HDAC4-GFP, and the fluorescence remained constant for 60 min. 1 μM staurosporine, a general kinase inhibitor, was then added to the same dishes without washing out of KN-62. The fluorescence signal was recorded for another 60 min. The same group of fibers that had no response to KN-62 subsequently responded to staurosporine, with a significant increase in nuclear HDAC4-GFP, indicating that staurosporine inhibition of a KN-62–insensitive kinase underlies the HDAC4 nuclear accumulation produced by staurosporine.

muscle activity to activate protein kinases or protein phosphatases, there was balanced unidirectional nuclear influx and efflux of HDAC4 at this rate to give zero net flux of HDAC4 since nuclear HDAC4 was constant in resting fibers under control conditions.

Next, we used FRAP to verify the existence of nuclear fluxes, and consequent nuclear shuttling of HDAC4 in unstimulated fibers under resting control conditions without pharmacological suppression of nuclear efflux by leptomycin B. The mean initial rate of recovery of nuclear fluorescence, determined by linear fit to the fluorescence during the first 30 min after photobleaching in each of six nuclei in six fibers, was 0.89 ± 0.15%/min. Subsequently, 120 min after photobleaching, leptomycin B was added to the same fibers and the mean rate of increase in nuclear fluorescence in the same fibers in the presence of leptomycin B was found to be 1.08 ± 0.18%/min. Thus the initial rate of HDAC4 fluorescence recovery in nuclei after near complete photobleaching was very similar to the rate of increase of nuclear fluorescence in the presence of leptomycin B, which is consistent with a resting nuclear influx (and efflux) equal to the rate of net nuclear influx seen in the presence of leptomycin B.

HDAC4 movements in resting fibers in the presence of protein kinase inhibitors

The CaMK inhibitor KN-62 completely blocked the net nuclear to cytoplasmic translocation of HDAC4-GFP in response to electrical stimulation (10-Hz trains; Fig. 2 C). Thus, we also explored the possible role of CaMK in the dynamic shuttling of HDAC4-GFP in resting fibers. During a 1-h period of exposure of unstimulated fibers to KN-62 (5 μM), the HDAC4-GFP fluorescence in the nucleus and in the cytoplasm were both stable, without any significant change (Fig. 8 C). This unexpected finding points out that although CaMK, inhibited by KN-62, played an essential role in calcium-triggered translocation of HDAC4-GFP out of nuclei during muscle activity (Figs. 1 and 2), any HDAC4 phosphorylation required for shuttling of HDAC4-GFP out of nuclei in unstimulated resting fibers was not mediated by CaMK, but may be mediated by another kinase.

To examine whether or not other protein kinases might affect the distribution of HDAC4-GFP in resting fibers, the broad-spectrum protein kinase inhibitor staurosporine was added to the same fibers that had been previously treated with KN-62 for 1 h. As shown in Fig. 8 C, staurosporine increased the fluorescence signal in the nucleus without affecting cytoplasmic fluorescence in the same unstimulated fibers that did not respond to KN-62. This finding demonstrates that there is one or more unidentified (non-CaMK) protein kinase controlling the shuttling of HDAC4-GFP in unstimulated fibers, whereas CaMK is activated and responsible for the Ca^{2+}-dependent increase in nuclear to cytoplasmic translocation of HDAC4 in stimulated fibers. Collectively, it seems that there are two different parallel biochemical pathways mediating HDAC4 phosphorylation before efflux from the nucleus, one that is activity and CaMK dependent and another that is activity and CaMK independent.

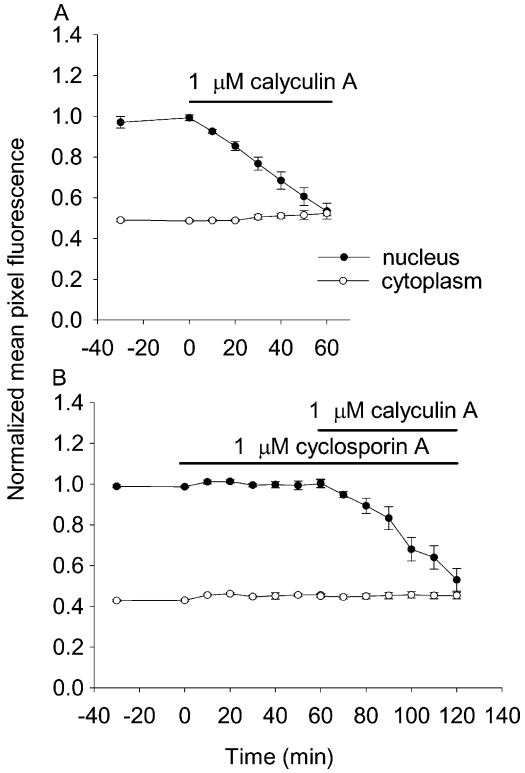

Figure 9. **Effects of protein phosphatase inhibitors on the subcellular distribution of HDAC4-GFP.** (A) The PP1 and PP2A inhibitor calyculin A dramatically decreased nuclear HDAC4-GFP in a 60-min period. HDAC4 nuclear and cytoplasmic fluorescence were constant during 30 min before calyculin A application. Calyculin A (final concentration 1 μM) caused a decline of nuclear fluorescence, but the cytoplasmic fluorescence remained constant. (B) 60-min exposure to the PP2B inhibitor CsA (1 μM) had no effect on nuclear fluorescence, whereas calyculin A subsequently decreased nuclear fluorescence in the same group of fibers.

Phosphatases mediating HDAC4 nuclear influx

Next, we tested the role of phosphatases in HDAC4 shuttling in resting fibers. Over a 60-min period of treatment with 1 μM calyculin A (a PP1 and PP2A phosphatase inhibitor that does not affect PP2B; Ishihara et al., 1989), the nuclear HDAC4-GFP fluorescence decreased linearly with a mean net export rate of −0.71 ± 0.07%/min (Fig. 9 A, 13 nuclei from 5 fibers). This rate is a measure of the net efflux with the calyculin A–sensitive endogenous phosphatases (PP1 and 2A) inhibited in the absence of muscle fiber activity and the resulting Ca^{2+}-dependent stimulation of kinases. Before addition of calyculin A, nuclear HDAC4 was constant, indicating that nuclear influx and efflux of HDAC4 were equal. The observed rate of efflux thus corresponds to the rate of PP1- and/or 2A-dependent HDAC4 influx into resting fibers. This rate is very similar to the rate of influx (0.88%/min) in the presence of leptomycin B, indicating that almost all of the influx of HDAC4 into nuclei during shuttling in resting fibers is mediated by PP1 or 2A dephosphorylation of HDAC4 in the cytoplasm. Interestingly, calyculin A also caused a similar rate of efflux of HDAC5-GFP (−0.62 ± 0.05, nine nuclei from six fibers) from nuclei as observed for HDAC4, establishing the ability of HDAC5 to move out of the nucleus even though it did not translocate in response to electrical stimulation.

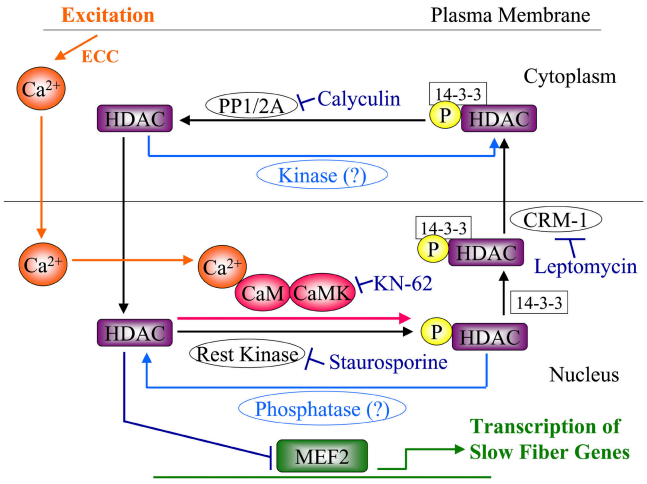

Figure 10. **Model of nuclear-cytoplasmic shuttling of HDAC4.** Nuclear shuttling of HDAC in resting muscle fibers at low cytosolic and nuclear Ca^{2+} concentration is based on its intra-nuclear phosphorylation, 14-3-3– and CRM1-dependent nuclear export, cytosolic dephosphorylation, and subsequent nuclear reentry. In response to muscle activity, cytosolic and nuclear Ca^{2+} concentration are elevated (orange), nuclear CaMK is activated (red), nuclear HDAC is phosphorylated, and the rate of HDAC efflux from the nucleus is consequently increased. The various inhibitors of kinases, phosphatases, and CRM1 used in this work are indicated in blue. Nuclear HDAC inhibits MEF2 transcriptional activation of slow fiber genes (green), and the activity-dependent efflux of HDAC from the nucleus removes this inhibition.

To rule out the possibility that PP2B (calcineurin) plays any role in the shuttling of HDAC4, we also studied the effects of cyclosporin A (CsA) on the distribution of HDAC4-GFP in resting fibers. 1 μM CsA had no effect on the distribution of HDAC4-GFP (Fig. 9 B). However, when calyculin A was subsequently added to the same culture, the nuclear HDAC4-GFP dropped significantly, at a net rate of -0.62 ± 0.13%/min (Fig. 9 B, seven nuclei from three fibers). Thus, the same fibers that exhibited no change in nuclear HDAC4-GFP in response to CsA did respond to block of PP1 and 2A by calyculin A with a robust decline in nuclear HDAC4-GFP.

Discussion

In the present work we have used virally expressed GFP and YFP fusion constructs to monitor and quantify the nuclear influx or efflux of the class II histone deacetylases HDAC4 and 5 and of CaM in adult skeletal muscle fibers maintained in culture. The novel findings of this work are: (a) activity-dependent net export of HDAC4 from the nucleus is mediated by CaMK; (b) CaMK activation during fiber stimulation occurs in the nucleus, without CaM-YFP translocation into the nucleus; and (c) activity-independent unidirectional efflux of HDAC4 from the nucleus occurs at a comparable rate in resting fibers as the activity-dependent net efflux during fiber stimulation but is mediated by a different as yet unknown kinase and is balanced by an equal rate of unidirectional influx of HDAC4 into the nucleus in resting fibers.

Class II HDACs are transcriptional regulators that suppress the activity of MEF2, a transcription factor involved in slow skeletal muscle fiber type gene expression. The components in the regulation of translocation of HDACs from the nucleus to the cytoplasm are shown in Fig. 10. Our results demonstrate that HDAC4 translocates out of the nucleus, presumably in complex with the chaperone protein 14-3-3 (Wang et al., 2000) in response to Ca^{2+} activation of CaM kinase in the nucleus during electrical stimulation (Fig. 10, orange and red). Unexpectedly, there is a relatively high rate of balanced nuclear influx and efflux of HDAC4 in resting, unstimulated fibers, resulting in shuttling of HDAC4 between the nucleus and the cytoplasm. Shuttling of HDAC4 in resting fibers was revealed by the influx of HDAC4-GFP in the presence of a blocker (leptomycin B) of the CRM1 efflux carrier, by the net nuclear efflux of HDAC4-GFP when cytosolic PP1 and 2A were blocked by calyculin A, and by the rate of HDAC4-GFP influx after FRAP. The unidirectional flux rates in resting fibers are coincidentally roughly about equal to the net rate of efflux in fibers stimulated with the 10-Hz train pattern (a 5-s duration 10-Hz train repeated every 50 s). Thus, the increased rate of efflux activated by fiber stimulation is only about equal in magnitude to the unidirectional flux rates in a resting fiber (i.e., stimulation approximately doubles the efflux rate).

By using two kinase inhibitors, KN-62 and staurosporine, we could demonstrate that different kinases underlie the activity-dependent net efflux activated in stimulated fibers and the unidirectional efflux underlying shuttling of HDAC4 in resting fibers. The activity-dependent net efflux is entirely blocked by the CaM kinase inhibitor KN-62, whereas the unidirectional efflux in resting fibers is not influenced by KN-62 but is inhibited by the broad-spectrum kinase inhibitor staurosporine (Fig. 10, added inhibitors shown in dark blue). These reciprocal pharmacological effects of two different kinase inhibitors demonstrate that different enzymes mediate HDAC4 efflux in resting fibers and the extra efflux activated in electrically stimulated fibers. There is no doubt that CaMK is a prominent kinase that phosphorylates HDAC4 and regulates its subcellular distribution (McKinsey et al., 2000b; Zhao et al., 2001). However, there are several reports suggesting that there are other protein kinases involved in HDAC phosphorylation and thereafter its subcellular distribution (Zhao et al., 2001). The binding of HDAC4 to 14-3-3 in U2OS cells is not stimulated by CaMK, and overexpression of CaMKIV did not increase HDAC4 binding to 14-3-3. Instead, there may be another kinase that phosphorylates HDAC4 and affects its subcellular distribution (Zhao et al., 2001). In cardiac muscle, an uncharacterized HDAC kinase is reported that is different from CaMK in response to specific inhibitors KN-62 or KN-93 (Zhang et al., 2002). Here, we show that the activity-dependent increase in HDAC4 phosphorylation by CaMK is approximately equal to the rate of HDAC4 phosphorylation by the unspecified kinase in resting fibers.

Our results also reveal that muscle fibers appear to exhibit isoform specificity in their handling of different members of class II HDACs. HDAC5-GFP was more highly concentrated in nuclei than HDAC4-GFP and did not exhibit stimulation-dependent nuclear efflux for stimulation patterns that clearly caused HDAC4 nuclear efflux, as previously observed in neurons (Chawla et al., 2003). However, both HDAC4 and 5 were de-

pleted from muscle nuclei at similar rates in the presence of calyculin A. Thus, these two HDACs respond similarly to phosphatase inhibition but differently to electrical stimulation.

Because CaMK underlies the activity-dependent efflux of HDAC4 from muscle fiber nuclei, we also used a virally expressed YFP construct of CaM to investigate if fiber electrical stimulation causes a net movement of CaM into the nuclei, as previously reported for high K^+ stimulation of hippocampal neurons (Deisseroth et al., 1998; Mermelstein et al., 2001). However, our results do not reveal any redistribution of CaM-YFP between the cytoplasm and the nucleus in response to the physiological patterns of action potential stimulation used here, even though our FRAP measurements demonstrate that CaM-YFP can move into nuclei relatively rapidly, likely via nuclear pores. Thus, the CaMK activation underlying the activity-dependent increase in nuclear kinase activity, and the resulting activity-dependent translocation of HDAC4 out of the nuclei, appears to be the result of CaMK activation by Ca^{2+} entry into the nuclei, the resulting binding of Ca^{2+} to CaM already present in the nuclei, and the consequent activation of nuclear CaMK (Fig. 10). In contrast, we did find that a large and prolonged elevation of Ca^{2+} in the presence of the Ca^{2+} ionophore ionomycin did cause an increase in the relative amount of CaM-YFP within the nuclei, but this change does not appear to be produced by the physiological electrical stimulation paradigm and is therefore not included in Fig. 10. Antibody staining revealed that the level of activated CaMKII in the nucleus increased with fiber stimulation, and that this increase was blocked by CaMK inhibitor KN-62, but that total nuclear CaMKII did not change with stimulation.

Finally, by using phosphatase inhibitors, we demonstrate that phosphatase 1 and/or 2A is likely involved in the cytoplasmic dephosphorylation and the resulting subsequent entry of HDAC4 into nuclei during shuttling in resting fibers, whereas the Ca^{2+}-dependent phosphase calcineurin does not appear to be involved in dephosphorylation of HDAC4 before nuclear entry (McKinsey et al., 2000a).

Comparison with earlier results and interpretations

The present paper presents the first study of the subcellular distribution of HDAC4 and HDAC5 in fully differentiated adult skeletal muscle fibers and of the changes in intracellular localization of HDAC4 in response to fiber stimulation. It s already known that CaMK plays an important role in the phosphorylation and exportation of HDAC4 from nuclei (McKinsey et al., 2000a, 2001) and that overexpression of active CaMK II or IV can facilitate the export of HDAC4 from the nucleus to the cytoplasm (Miska et al., 2001; Zhao et al., 2001). However, there are no previous studies using more physiological manipulations, which activate CaMK by directly increasing cytoplasmic and nuclear calcium in response to muscle fiber action potentials. Here, we demonstrate that electrical stimulation could result in net nuclear export of HDAC4 and that this transport was achieved by activating CaMK because the translocation was sensitive to the CaMK inhibitor KN-62.

Compared with our previous study of NFATc translocation in adult muscle fibers, the frequency-dependent translocation of HDAC4 is different from that of NFATc. 1-Hz stimulation is able to initiate export of HDAC4 out of the nucleus (present results), whereas 1-Hz stimulation had no effect on nuclear translocation of NFATc (Liu et al., 2001). This difference presumably reflects different responses of CaMK and calcineurin to the patterns of calcium transients. Both NFAT and HDAC are involved in the regulation of muscle fiber type. The calcineurin–NFATc pathway can up-regulate slow fiber type gene expression by NFAT binding to sites in the promotor region of slow fiber type–specific genes (Chin et al., 1998; Horsley and Pavlath, 2002). The CaMK–HDAC pathway may relieve the repression of MEF2 by HDAC (Miska et al., 1999), thereby allowing MEF2 to promote slower fiber type gene expression (Black and Olson, 1998; Wu et al., 2000). Thus, the responses to different frequencies noted here for the different gene regulation components HDAC4 and NFATc may provide an element of fine tuning for fiber type determination and transformation (Baldwin and Haddad, 2002; Spangenburg and Booth, 2003). Details of how the calcineurin–NFAT pathway may interrelate and "cross-talk" with the CaMK–HDAC pathway in skeletal muscle cells remain to be established (Chin, 2004).

There are numerous reports that in several kinds of cells CaM concentration in the nucleus increases in response to rinsing calcium (Deisseroth et al., 1998; Craske et al., 1999; Liao et al., 1999; Teruel et al., 2000; Mermelstein et al., 2001). Here, we tested the effects of electrical stimulation, which raises both cytoplasmic and nuclear calcium in muscle fibers. Surprisingly, neither 10-Hz trains nor 1-Hz continuous stimulation resulted in any changes in nuclear CaM-YFP in the adult skeletal muscle fibers used in this work. The difference from previous studies could result from different types of cells used or different kinds of stimuli. For example, here we used 10-Hz trains of 1-ms pulses to trigger muscle action potentials and initiate the resulting brief Ca^{2+} transients (Liu et al., 1997). In other studies, the elevated calcium could last from several seconds to several minutes (Teruel et al., 2000; Mermelstein et al., 2001), or even longer (Liao et al., 1999). In conclusion, stimulation-dependent activation of intranuclear CaMKII due to elevated nuclear Ca^{2+} appears to underlie the electrical stimulation–dependent efflux of HDAC4 from nuclei in adult muscle fibers.

Materials and methods

Construction of recombinant adenoviruses

The expression plasmid for HDAC4-GFP was a gift from S.L. Schreiber (Harvard University, Cambridge, MA; Grozinger and Schreiber, 2000). Production of recombinant adenovirus (Ad5) containing HDAC4-GFP cDNA, incorporation into pAdlox shuttle plasmid, and viral production by cre recombinase were performed according to the methods of Hardy et al. (1997) as previously described (Liu et al., 2001). Recombinant adenovirus expressing wild-type CaM-YFP was provided by D.T. Yue (Johns Hopkins University, Baltimore, MD; Erickson et al., 2001) and amplified using similar methods. A recombinant adenovirus containing a MEF2-luciferase reporter cassette, composed of six concatomerized MEF2 sites from the MCK muscle-specific enhancer upstream of a minimal TATA box-containing promoter, was provided by J.D. Molkentin (Children's Hospital Medical Center, Cincinnati, OH; Wilkins et al., 2004). Recombinant adenovirus expressing HDAC5-GFP was a gift from T.A. McKinsey (Myogen, Inc., Westminster, CO; Harrison et al., 2004).

Infection of recombinant adenoviruses in FDB fibers

Single muscle fibers were enzymatically dissociated from FDB muscles of 4–5-wk-old CD-1 mice and cultured as described previously (Liu et al., 1997). Isolated fibers were cultured on laminin-coated glass coverslips, each glued over a 10-mm-diam hole through the center of a plastic Petri dish (Liu et al., 1997). Fibers were cultured in MEM containing 10% FBS and 50 μg/ml of gentamicin sulfate in 5% CO_2 (37°C). Virus infections were performed as previously described (Liu et al., 2001).

Microscopy, image acquisition, and fiber stimulation

Approximately 72–76 h after infection, culture medium was changed to Ringer's solution (135 mM NaCl, 4 mM KCl, 1 mM $MgCl_2$, 10 mM Hepes, 10 mM glucose, and 1.8 mM $CaCl_2$, pH 7.4). The culture chamber was mounted on an inverted microscope (model IX70; Olympus) equipped with a laser scanning confocal imaging system (model MRC-600; Bio-Rad Laboratories) using an argon ion laser supplying an excitation wavelength of 488 nm. Fibers were viewed with a 60×/1.4 NA water immersion objective (Olympus) and scanned at 1.6× zoom using constant laser power and gain. Two platinum electrodes connected to a stimulator were placed into the fiber culture chamber to give field stimulation. The fibers were maintained and imaged at RT (24°C) for 30 min before the stimulation began, after which the focus was adjusted to obtain a sharp view of the previously imaged nuclei. The duration of the individual stimulating pulses was 1 ms in all protocols. The stimulation voltage was adjusted to give microscopically observed fiber contraction in all cases. Most fibers remained attached to the laminin-coated coverslip throughout the period of fiber stimulation and recovery, and only such fibers were used to obtain the data reported here. Confocal images were taken at regular intervals before, during, and after stimulation.

For treatment with chemical reagents, fibers were rinsed with Ringer's solution and a first (control) image was taken. The cultures were maintained on the microscope stage for 30 min (−30 min in the figures) before the chemical reagents were added. One image was taken immediately after drug addition (0 min in the figures), and then images were taken every 10 min. Leptomycin B, calyculin A, and staurosporine were purchased from LC Laboratories. KN-62 was purchased from Calbiochem.

Analysis of translocation of GFP- or YFP-tagged proteins in living fibers

The average fluorescence of pixels within user-specified areas of interest (AOI) in each image were quantitated using software custom-written in the IDL programming language (Research Systems). For each electrical stimulation or pharmacological experiment, the time course of the average pixel fluorescence within each AOI was first fitted with a straight line, from which a predicted time 0 value was obtained. Then, all the fluorescence values for the AOI at each time point were divided (normalized) by the predicted time zero value for the AOI. The resulting data gives the relative value of fluorescence of each individual AOI at different time points normalized to the predicted time 0 value in the same AOI. This method was used throughout all the experimental groups. Results are expressed as the mean ± SEM. The rate of change (percent per min) of fluorescence was calculated from the slope of the linear fit through the normalized fluorescence data for each nuclear or each cytoplasmic AOI. Note that such calculated rates of change of fluorescence are relative to the initial fluorescence within each AOI as determined by the linear fit to the fluorescence values over the initial time interval.

Nuclear FRAP

FRAP experiments were performed on a confocal microscope (model Fluoview 500; Olympus). The GFP or YFP moiety was excited at 488 or 514 nm and emission was detected at above 505 or at 535–565 nm, respectively. After recording a prebleach image, a rectangular region slightly larger than the nucleus and covering the entire nucleus was scanned/photobleached with maximum laser power. Subsequently, images were captured at 10-min intervals for 60 min at lower laser power. During recording of the prebleach and time-lapse recovery images, no significant photobleaching was observed. The change in mean nuclear pixel fluorescence over time was quantified by IDL program, and then it was fitted to $F(t) = F_0 + a(1 - e^{-kt})$, where F(t) and F_0 are the nuclear fluorescence at time t or at time 0 after bleach, respectively; k is the rate constant of fluorescence recovery after bleach, which is a measurement of fluorescent protein (HDAC4-GFP or CaM-YFP) influx from the cytoplasm to the nucleus; and $F_0 + a$ is the final fluorescence attained after recovery from photobleaching.

MEF2 activity and CaMK phosphorylation

For MEF2 reporter or CaMK phosphorylation studies, FDB fibers cultured in coverslip-bottomed wells in culture dishes with two stainless steel wire electrodes glued to the bottom of the dish (Liu and Schneider, 1998) were repetitively stimulated.

CaMKII autophosphorylation at Thr-286 (287) was analyzed by immunofluorescence stain after fixation and permeabilization (Liu et al., 2001) using a phospho-specific antibody that recognizes CaMKII only when it is autophosphorylated at Thr-286 (α) or Thr-287 (β, γ, and δ) (Promega; Chang et al., 1998; Rose and Hargreaves, 2003) or with antibody directed against total CaMKII (Chemicon), both detected with Cy5-conjugated second antibody. The fluorescence of the nucleus in the stained fibers was quantified using the confocal microscope (Olympus) with constant laser power and gain.

To measure MEF2 reporter activity, the cultures were lysed in passive lysis buffer (Promega). Luciferase activity was determined with the luciferase assay kit (Promega).

Calcium recording

Culture medium was first changed to normal Ringer's solution. Fluo-4AM in DMSO was added to dishes to give a final concentration of 2 μM fluo-4AM in Ringer's solution. After loading for 20 min, cultures were rinsed three times with Ringer's solution and equilibrated for 20 min before recording. The fibers were stimulated with the same stimulator as used for studying HDAC4-GFP translocation. The pulse generator was precisely synchronized with the confocal microscope during image acquisition. Dye loading and calcium recording were performed at RT (24°C).

We thank Dr. S.L. Schreiber for HDAC4-GFP cDNA, Dr. D.T. Yue for adenovirus encoding CaM-YFP, Dr. J.D. Molkentin for adenovirus encoding MEF2-luciferase reporter, Dr. T.A. McKinsey for adenovirus encoding HDAC5-GFP, and Ms. Kara Franz and Ms. Carrie Wagner for technical assistance.

This work was supported by National Institutes of Health grant R01-NS33578 from The National Institute of Neurological Disorders and Stroke.

Submitted: 23 August 2004
Accepted: 25 January 2005

References

Baldwin, K.M., and F. Haddad. 2002. Skeletal muscle plasticity: cellular and molecular responses to altered physical activity paradigms. *Am. J. Phys. Med. Rehabil.* 81:S40–S51.

Black, B.L., and E.N. Olson. 1998. Transcriptional control of muscle development by myocyte enhancer factor-2 (MEF2) proteins. *Annu. Rev. Cell Dev. Biol.* 14:167–196.

Chang, B.H., S. Mukherji, and T.R. Soderling. 1998. Characterization of a calmodulin kinase II inhibitor protein in brain. *Proc. Natl. Acad. Sci. USA.* 95:10890–10895.

Chawla, S., P. Vanhoutte, F.J. Arnold, C.L. Huang, and H. Bading. 2003. Neuronal activity-dependent nucleocytoplasmic shuttling of HDAC4 and HDAC5. *J. Neurochem.* 85:151–159.

Chin, E.R. 2004. The role of calcium and calcium/calmodulin-dependent kinases in skeletal muscle plasticity and mitochondrial biogenesis. *Proc. Nutr. Soc.* 63:279–286.

Chin, E.R., E.N. Olson, J.A. Richardson, Q. Yang, C. Humphries, J.M. Shelton, H. Wu, W. Zhu, R. Bassel-Duby, and R.S. Williams. 1998. A calcineurin-dependent transcriptional pathway controls skeletal muscle fiber type. *Genes Dev.* 12:2499–2509.

Craske, M., T. Takeo, O. Gerasimenko, C. Vaillant, K. Torok, O.H. Petersen, and A.V. Tepikin. 1999. Hormone-induced secretory and nuclear translocation of calmodulin: oscillations of calmodulin concentration with the nucleus as an integrator. *Proc. Natl. Acad. Sci. USA.* 96:4426–4431.

Deisseroth, K., H. Bito, and R.W. Tsien. 1996. Signaling from synapse to nucleus: postsynaptic CREB phosphorylation during multiple forms of hippocampal synaptic plasticity. *Neuron.* 16:89–101.

Deisseroth, K., E.K. Heist, and R.W. Tsien. 1998. Translocation of calmodulin to the nucleus supports CREB phosphorylation in hippocampal neurons. *Nature.* 392:198–202.

Erickson, M.G., B.A. Alseikhan, B.Z. Peterson, and D.T. Yue. 2001. Preassociation of calmodulin with voltage-gated Ca^{2+} channels revealed by FRET in single living cells. *Neuron.* 31:973–985.

Fukuda, M., S. Asano, T. Nakamura, M. Adachi, M. Yoshida, M. Yanagida, and E. Nishida. 1997. CRM1 is responsible for intracellular transport mediated by the nuclear export signal. *Nature.* 390:308–311.

Grozinger, C.M., and S.L. Schreiber. 2000. Regulation of histone deacetylase 4 and 5 and transcriptional activity by 14-3-3-dependent cellular localization. *Proc. Natl. Acad. Sci. USA.* 97:7835–7840.

Hardy, S., M. Kitamura, T. Harris-Stansil, Y. Dai, and M.L. Phipps. 1997. Con-

struction of adenovirus vectors through Cre-lox recombination. *J. Virol.* 71:1842–1849.

Harrison, B.C., C.R. Roberts, D.B. Hood, M. Sweeney, J.M. Gould, E.W. Bush, and T.A. McKinsey. 2004. The CRM1 nuclear export receptor controls pathological cardiac gene expression. *Mol. Cell. Biol.* 24:10636–10649.

Hennig, R., and T. Lomo. 1985. Firing patterns of motor units in normal rats. *Nature.* 314:164–166.

Horsley, V., and G.K. Pavlath. 2002. NFAT: ubiquitous regulator of cell differentiation and adaptation. *J. Cell Biol.* 156:771–774.

Ishihara, H., B.L. Martin, D.L. Brautigan, H. Karaki, H. Ozaki, Y. Kato, N. Fusetani, S. Watabe, K. Hashimoto, D. Uemura, et al. 1989. Calyculin A and okadaic acid: inhibitors of protein phosphatase activity. *Biochem. Biophys. Res. Commun.* 159:871–877.

Kao, H. Y., A. Verdel, C. C. Tsai, C. Simon, H. Juguilon, and S. Khochbin. 2001. Mechanism for nucleocytoplasmic shuttling of histone deacetylase 7. *J. Biol. Chem.* 276:47496–47507.

Kirsh, O., J.S. Seeler, A. Pichler, A. Gast, S. Muller, E. Miska, M. Mathieu, A. Harel-Bellan, T. Kouzarides, F. Melchior, and A. Dejean. 2002. The SUMO E3 ligase RanBP2 promotes modification of the HDAC4 deacetylase. *EMBO J.* 21:2682–2691.

Liao, B., B.M. Paschal, and K. Luby-Phelps. 1999. Mechanism of Ca^{2+}-dependent nuclear accumulation of calmodulin. *Proc. Natl. Acad. Sci. USA.* 96:6217–6222.

Liu, Y., and M.F. Schneider. 1998. Fibre type-specific gene expression activated by chronic electrical stimulation of adult mouse skeletal muscle fibres in culture. *J. Physiol.* 512:337–344.

Liu, Y., S.L. Carroll, M.G. Klein, and M.F. Schneider. 1997. Calcium transients and calcium homeostasis in adult mouse fast-twitch skeletal muscle fibers in culture. *Am. J. Physiol.* 272:C1919–C1927.

Liu, Y., Z. Cseresnyes, W.R. Randall, and M.F. Schneider. 2001. Activity-dependent nuclear translocation and intranuclear distribution of NFATc in adult skeletal muscle fibers. *J. Cell Biol.* 155:27–39.

Lu, J., T.A. McKinsey, R.L. Nicol, and E.N. Olson. 2000. Signal-dependent activation of the MEF2 transcription factor by dissociation from histone deacetylases. *Proc. Natl. Acad. Sci. USA.* 97:4070–4075.

McKinsey, T.A., C.L. Zhang, J. Lu, and E.N. Olson. 2000a. Signal-dependent nuclear export of a histone deacetylase regulates muscle differentiation. *Nature.* 408:106–111.

McKinsey, T.A., C.L. Zhang, and E.N. Olson. 2000b. Activation of the myocyte enhancer factor-2 transcription factor by calcium/calmodulin-dependent protein kinase-stimulated binding of 14-3-3 to histone deacatylase 5. *Proc. Natl. Acad. Sci. USA.* 97:14400–14405.

McKinsey, T.A., C.L. Zhang, and E.N. Olson. 2001. Identification of a signal-responsive nuclear export sequence in class II histone deacetylases. *Mol. Cell. Biol.* 21:6312–6321.

Mermelstein, P.G., K. Deisseroth, N. Dasgupta, A.L. Isaksen, and R.W. Tsien. 2001. Calmodulin priming: nuclear translocation of a calmodulin complex and the memory of prior neuronal activity. *Proc. Natl. Acad. Sci. USA.* 98:15342–15347.

Miska, E.A., C. Karlsson, E. Langley, S.J. Nielsen, J. Pines, and T. Kouzarides. 1999. HDAC4 deacetylase associates with and represses the MEF2 transcription factor. *EMBO J.* 18:5099–5107.

Miska, E.A., E. Langley, D. Wolf, C. Karlsson, J. Pines, and T. Kouzarides. 2001. Differential localization of HDAC4 orchestrates muscle differentiation. *Nucleic Acids Res.* 29:3439–3447.

Rose, A.J., and M. Hargreaves. 2003. Exercise increases Ca^{2+}-calmodulin-dependent protein kinase II activity in human skeletal muscle. *J. Physiol.* 553:303–309.

Spangenburg, E.E., and F.W. Booth. 2003. Molecular regulation of individual skeletal muscle fibre types. *Acta Physiol. Scand.* 178:413–424.

Teruel, M.N., W. Chen, A. Persechini, and T. Meyer. 2000. Differential codes for free Ca^{2+}-calmodulin signals in nucleus and cytosol. *Curr. Biol.* 10: 86–94.

Tokumitsu, H., T. Chijiwa, M. Hagiwara, A. Mizutani, M. Terasawa, and H. Hidaka. 1990. KN-62, 1-[N,O-bis(5-isoquinolinesulfonyl)-N-methyl-L-tyrosyl]-4-phenylpiperazine, a specific inhibitor of Ca^{2+}/calmodulin-dependent protein kinase II. *J. Biol. Chem.* 265:4315–4320.

Van Hemert, M.J., H.Y. Steensma, and G.P.H. Van Heusden. 2001. 14-3-3 proteins: key regulators of cell division, signaling and apoptosis. *Bioessays.* 23:936–946.

Wang, A.H., M.J. Kruhlak, J. Wu, N.R. Bertos, M. Vezmar, B.I. Posner, D.P. Bazett-Jones, and X.J. Yang. 2000. Regulation of histone deacetylase 4 by binding of 14-3-3 proteins. *Mol. Cell. Biol.* 20:6904–6912.

Wilkins, B.J., Y.S. Dai, O.F. Bueno, S.A. Parsons, J. Xu, D.M. Plank, F. Jones, T.R. Kimball, and J.D. Molkentin. 2004. Calcineurin/NFAT coupling participates in pathological, but not physiological, cardiac hypertrophy. *Circ. Res.* 94:110–118.

Wu, H., F.J. Naya, T.A. McKinsey, B. Mercer, J.M. Shelton, E.R. Chin, A.R. Simard, R.N. Michel, R. Bassel-Duby, E.N. Olson, and R.S. Williams. 2000. MEF2 responds to multiple calcium-regulated signals in the control of skeletal muscle fiber type. *EMBO J.* 19:1963–1973.

Zhang, C.L., T.A. McKinsey, S. Chang, C.L. Antos, J.A. Hill, and E.N. Olson. 2002. Class II histone deacetylases act as signal-responsive repressors of cardiac hypertrophy. *Cell.* 110:479–488.

Zhao, X., A. Ito, C.D. Kane, T.S. Liao, T.A. Bolger, S.M. Lemrow, A.R. Means, and T.P. Yao. 2001. The modular nature of histone deacetylase HDAC4 confers phosphorylation-dependent intracellular trafficking. *J. Biol. Chem.* 276:35042–35048.